

| Topic | Determination of fault-plane solutions |
|---------|--|
| Authors | Michael Baumbach  , and Peter Bormann (formerly GeoForschungsZentrum Potsdam, Department 2: Physics of the Earth, Telegrafenberg, D-14473 Potsdam, Germany); E-mail: pb65@gmx.net |
| Version | September 1999 |

1 Aim

The exercise aims at:

- understanding how fault slip affects the polarities of P waves;
- understanding the presentation of P-wave polarities in an equal angle (Wulff net) or equal area projection (Lambert-Schmidt net) of the focal sphere;
- constructing a fault-plane solution and determining the related parameters (**P** and **T** axes, displacement vector) for a real earthquake;
- relating the directions of the fault-plane solutions to the tectonic setting.

2 Data and procedures

Before a fault-plane solution for a teleseismic event can be constructed, the following steps must be completed:

- Interpretation of P-wave first-motion polarities from seismograms at several stations;
- Calculation of epicentral distances and source-to-station azimuths for these stations;
- Calculation of the take-off angles for the seismic P-wave rays leaving the hypocenter towards these stations. This requires the knowledge of the focal depth and of the P-wave velocity at this depth (see EX 3.3).

For the calculations b) and c) standard Earth velocity models are used (e.g., Kennett, 1991).

In the case of local events it is necessary to determine which branch of the travel-time curve is arriving first. The events should be located, if possible, with a special layered crustal velocity model for that region. Most such programs provide both the source-station azimuths and take-off angles in their output files.

The exercise below is based on the definitions, relationships and diagrams (Figs. 3.27 – 3.33) given in the NMSOP, Chapter 3, section 3.4.2 “Manual determination of fault-plane solutions.”. As an example consider the data in Table 1 that was determined following steps a)-c), by using the program HYPO71, for a locally recorded aftershock of the Erzincan earthquake in Turkey (Date: 12.04.1992, $M_l = 2.8$, latitude = 39.519° N, longitude = 39.874° E, source depth $h = 3$ km; station distance up to 50 km).

Note: The take-off angles, AIN, calculated for a ray arriving at a given seismic station may vary significantly depending on the assumed velocity model in the source region. Also, for an average single layer crustal model of 30 to 40 km thickness, all P-wave first arrivals within a distance of about 120 - < 200 km are Pg and up-going. That is, they emerge only from the upper half of the focal hemisphere. Also, when using HYPO71 with the average global two-layer crust according to the velocity model IASP91 (Kenneth 1991) only upper hemisphere take-off angles would have been calculated for the first P-wave arrivals up to distances of 50 km. But in the epicentral area under consideration a significant velocity increase in the upper

crust was already found at 4 km depth (increase of $v_p = 5.3$ km/s to 6.0 km/s). Accordingly, stations up to 50 km distance were reached by upper or lower focal sphere rays (see Fig. 3.29). Since only lower hemisphere projections will be used in the exercise values, for upper hemisphere rays ($AIN > 90^\circ$) must be corrected according to Fig. 3.28. **Conclusion:** AIN calculations based on strongly biased velocity models might result in inconsistent fault-plane solutions or not permit a proper separation of polarity readings into quadrants at all!

Table 1 gives the needed primary data. They were taken from the output file of the program HYPO71 with which the event was located. The first five columns of this file contain, as an example for the two stations ALI and ESK in Tab. 1, the following data:

| STN | DIST | AZM | AIN | PRMK |
|-----|------|-----|-----|------|
| ALI | 3.7 | 40 | 130 | IPD0 |
| ESK | 22.7 | 312 | 62 | IPU1 |

with STN - station code; DIST - epicentral distance in km; AZM - azimuth towards the station clockwise in degree from north; AIN - take-off angle of the ray towards the station, measured as in Fig. 3.28, and calculated for the given structure-velocity model; PRMK - P-wave reading remarks. In the column PRMK P stands for P-wave onset, I for impulsive (sharp) or E for emergent (less clear) onset, D for clear (or - for poor) dilatational (downward) first motion, U for clear (or + for poor) compressional (upward) first motion as read at the station. The last character may range between 0 and 4 and is a measure of the quality (clarity) of the onset and thus of the weight given to the reading in the calculation procedure, e.g., 4 for zero and 0 for full weight. In case of the above two stations the values for ALI would need to be corrected to get the respective values for the equivalent lower hemisphere ray, i.e., $AINc = 180^\circ - 130^\circ = 50^\circ$ and $AZMc = 180^\circ + 40^\circ = 220^\circ$ while the values for ESK can be taken unchanged from the HYPO71 output file.

3 Tasks

Task 1:

If in Table 1 $AIN > 90^\circ$, then correct take-off angles and azimuths for lower hemisphere projection: $AINc = 180^\circ - AIN$, $AZMc = AZM(<180^\circ) + 180^\circ$ or $AZM(\geq 180^\circ) - 180^\circ$. In case of $AIN < 90^\circ$ the original values remain unchanged.

Task 2:

Place tracing paper or a transparency sheet over the Wulff or Lambert-Schmidt net projection (see Fig. 3.27a or b in 3.4.2). Mark on it the center and perimeter of the net as well as the N, E, S and W directions. Pin the marked sheet center with a needle to the center of the net.

Task 3:

Mark the azimuth of the station on the perimeter of the transparency and rotate the latter until the tick mark is aligned along an azimuth of 0° , 90° , 180° or 270° . Measure the take-off angle from the center of the net along this azimuth. This gives the intersection point of the particular P-wave ray with the lower hemisphere. Mark on this position the P-wave polarity with a neat + for compression or o for dilatation (U or D in Tab. 1) using *different colors* for better distinction of closely spaced polarities of different sign. **Note:** The proper distance (d) of the polarity entry from the center of the net corresponds to $d = r \times \tan(AIN / 2)$ for the Wulff net and $d = r \times \sin(AIN / 2)$ for the Lambert-Schmidt net with r the radius of the given net. In

case that rays left the source through the upper hemisphere ($AIN > 90^\circ$) $AINc$ for lower hemisphere projection has to be calculated and used!

Table 1 Original and corrected values of ray azimuth (AZM and AZMc) and take-off angles (AIN and AINc) towards stations of a temporary network which recorded the Erzincan aftershock of April 12, 1994. POL - polarity of P-wave first motions.

| STA | AZM (degree) | AIN (degree) | POL | AZMc (degree) | AINc (degree) |
|-----|-----------------|-----------------|-----|------------------|------------------|
| ALI | 40 | 130 | D | | |
| ME2 | 134 | 114 | D | | |
| KAN | 197 | 112 | D | | |
| YAR | 48 | 111 | D | | |
| ERD | 313 | 103 | D | | |
| DEM | 330 | 102 | D | | |
| GIR | 301 | 102 | U | | |
| UNK | 336 | 101 | D | | |
| SAN | 76 | 62 | U | | |
| PEL | 327 | 62 | D | | |
| GUN | 290 | 62 | U | | |
| ESK | 312 | 62 | U | | |
| SOT | 318 | 62 | D | | |
| BA2 | 79 | 62 | U | | |
| MOL | 297 | 62 | U | | |
| YUL | 67 | 62 | U | | |
| ALT | 59 | 62 | D | | |
| GUM | 320 | 62 | U | | |
| GU2 | 320 | 62 | D | | |
| BAS | 308 | 62 | D | | |
| BIN | 295 | 62 | U | | |
| HAR | 24 | 62 | D | | |
| KIZ | 311 | 62 | U | | |
| AKS | 284 | 62 | D | | |
| SUT | 295 | 62 | U | | |

Task 4:

By rotating the transparent sheet with the plotted data over the net try to find a great circle which separates as good as possible the expected quadrants with different first motion signs. This great circle represents the intersection trace of one of the possible fault (or nodal) planes (FP1) with the lower half of the focal sphere. **Note 1:** All N-S connecting lines on both nets are great circles! **Note 2:** Inconsistent polarities that are close to each other may be due to uncertainty in reading relatively small P-wave amplitudes. The phenomenon occurs

particularly for take-off angles near nodal (fault) planes. Thus, clusters of inconsistent polarities may guide you in finding the best separating great circle. However, be aware that isolated inconsistent polarities might be due to false polarity switching or erroneous first motion polarity reading at the seismic station.

Task 5:

Mark point A at the middle of FP1 and find, on the great circle perpendicular to it, the pole P1 of FP1, 90° apart (see Fig. 3.31). All great circles, passing this pole are perpendicular to the FP1. Since the second possible fault plane (FP2) must be perpendicular to the FP1, it has to pass P1. Find, accordingly, FP2 which again has to separate areas of different polarity.

Task 6:

Find the pole P2 for FP2 (which is on FP1!) and delineate the equatorial plane EP. The latter is perpendicular to both FP1 and FP2, i.e., a great circle through the poles P1 and P2. The intersection point of FP1 and FP2 is the pole of the equatorial plane (P3).

Task 7:

Mark the position of the poles of the pressure (**P**) and tension axes (**T**) on the equatorial plane and determine the direction of these axes towards (for **P**) and away from the center (for **T**) of the used net (see Fig. 3.31). The poles for **P** and **T** lie on the equatorial plane in the center of the respective quadrants of dilatational (-) and compressional (+) P-wave first motions, i.e., 45° away from the intersection points of the two fault planes with the equatorial plane. **Note:**

All angles in the net projections have to be measured along great circles!

Task 8:

Mark the slip vectors, connecting the intersection points of the fault planes with the equatorial plane, with the center of the considered net. If the center lies in a tension quadrant, then the slip vectors point to the net center (see Fig. 3.31). If it lies in a pressure quadrant, then the slip vector points in the opposite direction. The slip vector shows the direction of displacement of the hanging wall.

Task 9:

Determine the azimuth (strike direction ϕ) of both FP1 and FP2. It is the angle measured clockwise against North between the directional vector connecting the center of the net with the end point of the respective projected fault trace lying towards the right of the net center (i.e., with the fault plane dipping towards the right; see Fig. 3.31).

Task 10:

Determine the dip angle δ (measured from horizontal) for both FP1 and FP2 by putting their projected traces on a great circle. Measure δ as the difference angle from the outermost great circle towards the considered fault-plane trace.

Task 11:

Determine the slip direction (i.e., the sense of motion along the two possible fault planes. It is obtained by drawing one vector each from the center of the net to the poles P1 and P2 of the nodal planes (or vice versa from the poles to the center depending on the sign of the rake

angle λ). The vector from (or to) the center to (or from) P1 (P2) shows the slip direction along FP2 (FP1). The rake angle λ is positive in case the center of the net lies in the tension (+) quadrant (i.e., an event with a thrust component) and negative when it lies in the pressure (-) quadrant (event with a normal faulting component). In the first case λ is $180^\circ - \lambda^*$. λ^* has to be measured on the great circle of the respective fault plane between its crossing point with the equatorial plain and the respective azimuth direction of the considered fault plane (see Fig. 3.31). In the second case $\lambda = -\lambda^*$. For a pure strike slip motion ($\delta = 90^\circ$) $\lambda = 0$ defines a left lateral strike-slip and $\lambda = 180^\circ$ defines a right-lateral strike-slip.

Task 12:

The azimuth of the pressure and the tension axes, respectively, is equal to the azimuth of the line connecting the center of the net through the poles of **P** and **T** with the perimeter of the net. Their plunge is the dip angle of these vectors against the horizontal (to be measured as for δ).

Task 13:

Estimate the parameters of the fault planes and of the pressure and tension axes for the Erzincan aftershock and insert your results into Table 2 below:

Table 2

| | strike | dip | rake |
|---------------|--------|-----|------|
| Fault plane 1 | | | |
| Fault plane 2 | | | |

| | azimuth | plunge |
|---------------|---------|--------|
| Pressure axis | | |
| Tension axis | | |

Note: The angles may range between:

- $0^\circ < \text{strike} < 360^\circ$
- $0^\circ < \text{azimuth} < 360^\circ$
- $0^\circ < \text{dip} < 90^\circ$
- $0^\circ < \text{plunge} < 90^\circ$
- $-180^\circ < \text{rake} < 180^\circ$

Task 14:

The question of which of the nodal planes was the active fault plane, and hence the other was the auxiliary plane, cannot be answered on the basis of the fault-plane solution alone.

Considering the event in its seismotectonic context may give an answer. Therefore, we have marked the epicenter of the event in Figure 1 with an open star at the secondary fault F2.

- a) Decide which was the likely fault plane (FP1 or FP2)?
- b) What was the type of faulting?
- c) What was the direction of slip? and

- d) Is your solution compatible with the general sense of plate motion in the area as well with the orientation of the acting fault and the orientation of stress/deformation in the area?

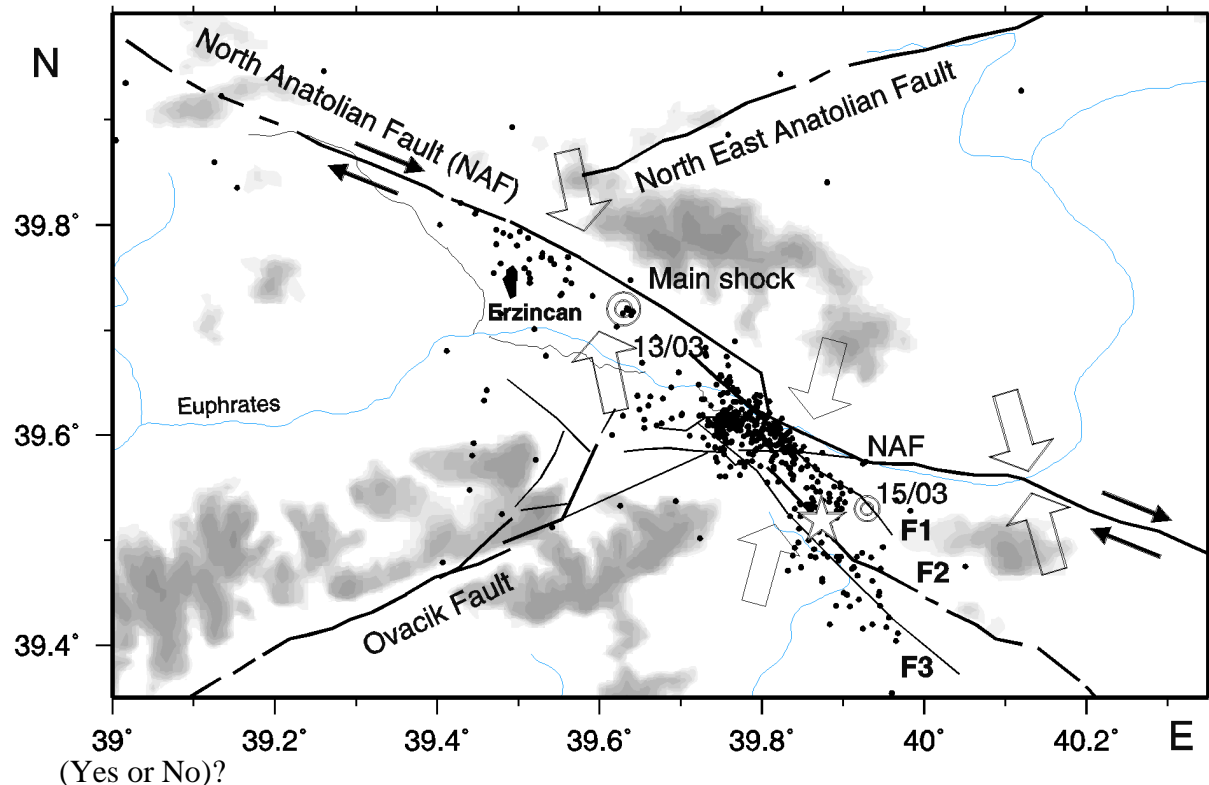


Figure 1 Epicenters of aftershocks between March 21 and June 16, 1992 of the March 13, 1992 Erzincan earthquake, Turkey. The open circles represent the main shock and its strongest aftershock on March 15, and the open star the analyzed aftershock. **F1**, **F2** and **F3** are secondary faults to the North Anatolian Fault (NAF). Black arrows - directions of relative plate motion, open arrows - direction of maximum horizontal compression as derived from centroid moment-tensor solutions of stronger earthquakes (courtesy of H. Grosser).

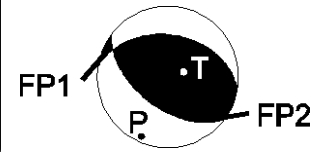
4 Solutions

In the Table 3 below the authors have given the data for their own freehand fits together with the values for the best PC fit to the data (in brackets). If your manually determined results differ by more than about 20° or even show a different type of faulting mechanism, you should critically check your data entries and/or fault-plane fits again.

Table 3

| | strike | dip | rake |
|---------------------|-------------------------------|-----------------------------|-------------------------------|
| Fault plane 1 (FP1) | 280° (278.5°) | 40° (39.9°) | 68° (67.4°) |
| Fault plane 2 (FP2) | 130° (127.0°) | 54° (53.7°) | 108° (107.8°) |

| | azimuth | plunge |
|---------------|---------------|-------------|
| Pressure axis | 205° (204.4°) | 7° (7.1°) |
| Tension axis | 90° (88.6°) | 73° (74.0°) |



The answers to the questions in Task 14 are:

- FP2 was more likely the active fault.
- The aftershock was a thrust event with a very small right-lateral strike-slip component.
- The slip direction is here strike - rake azimuth, i.e., for FP2 $130^\circ - 108^\circ = 12^\circ$ from north. This is close to the direction of maximum horizontal compression (15°) in the nearby area as derived from centroid moment-tensor solutions of stronger events.
- The strike of FP2 for this event agrees with the general direction of mapped surface fault strike and is consistent with the tendency of plate motion direction in the area under study. Therefore, it is highly probable that FP2 was the acting fault.

